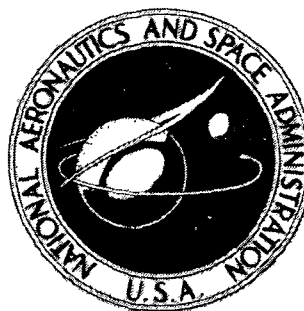


N73-18573

NASA TECHNICAL
MEMORANDUM



NASA TM X-2750

NASA TM X-2750

CASE FILE
COPY

AN EXPLORATORY STUDY
OF THE MICROSTRUCTURE
OF MULLITE FIBERS

*by Gilbert J. Santoro, Hubert B. Probst,
and Bruno C. Buzek*

*Lewis Research Center
Cleveland, Ohio 44135*

1. Report No. NASA TM X-2750		2. Government Accession No.		3. Recipient's Catalog No.	
4. Title and Subtitle AN EXPLORATORY STUDY OF THE MICROSTRUCTURE OF MULLITE FIBERS				5. Report Date March 1973	
				6. Performing Organization Code	
7. Author(s) Gilbert J. Santoro, Hubert B. Probst, and Bruno C. Buzek				8. Performing Organization Report No. E-7253	
				10. Work Unit No. 502-31	
9. Performing Organization Name and Address Lewis Research Center National Aeronautics and Space Administration Cleveland, Ohio 44135				11. Contract or Grant No.	
				13. Type of Report and Period Covered Technical Memorandum	
12. Sponsoring Agency Name and Address National Aeronautics and Space Administration Washington, D. C. 20546				14. Sponsoring Agency Code	
15. Supplementary Notes					
16. Abstract Mullite fibers of three compositions, ranging from SiO ₂ -rich to Al ₂ O ₃ -rich, were investigated by a number of transmission electron microscopy (TEM) techniques. The fibers were examined in the as-received condition and after subjecting them to thermal exposures as high as 1426° C. The investigative techniques used included direct TEM of microtomed sections of mounted fibers and TEM of replicas of polished, chemically etched, and cathodically etched fibers. In addition, X-ray diffraction line broadening analyses was used for determining average crystallite size. A preliminary description of the microstructure of mullite fibers is given.					
17. Key Words (Suggested by Author(s)) Ceramic fibers Insulation Reusable surface insulation Mullite				18. Distribution Statement Unclassified - unlimited	
19. Security Classif. (of this report) Unclassified		20. Security Classif. (of this page) Unclassified		21. No. of Pages 25	
				22. Price* \$3.00	

* For sale by the National Technical Information Service, Springfield, Virginia 22151

AN EXPLORATORY STUDY OF THE MICROSTRUCTURE OF MULLITE FIBERS

by Gilbert J. Santoro, Hubert B. Probst, and Bruno C. Buzek

Lewis Research Center

SUMMARY

In this investigation the microstructure of three mullite-composition fibers were examined by a number of transmission electron microscopy (TEM) techniques. The standard composition was slightly Al_2O_3 -rich; it is presently being used in the fabrication of rigidized tiles - a concept to provide lightweight thermal protection for re-entry vehicles. Of the other two compositions, one was highly Al_2O_3 -rich and the other was SiO_2 -rich. The fibers were examined in the as-received condition and after subjecting them to thermal exposures in air as high as 1426°C . The investigative techniques used included direct TEM of microtomed sections of mounted fibers and TEM of replicas of polished, chemically etched, and cathodically etched fibers. In addition X-ray diffraction line broadening analyses was used for determining average crystallite size.

The as-received fibers of standard composition (both spun and monofilament) contained little if any internal porosity. Nor did the degree of porosity increase after heating the monofilament for 1/2 hour at 1205°C . Prior to the thermal exposures the crystallites in all three of the spun fibers (standard, alumina-rich, and silica-rich) were very small (about 100×10^{-10} to 200×10^{-10} m or 100 to 200 Å) and were dispersed in a large amount of an amorphous phase. When thermally exposed, these crystallites grew and simultaneously new crystallites were nucleated from the amorphous phase. After sufficient time at temperature (e.g., 116 hr at 1426°C), the crystallites of the standard spun fibers became contiguous. At this juncture the average crystallite size was less than 0.2 micrometer, relatively small compared to the mean fiber diameter of 6.8 micrometers. In addition, the surface crystallites of these fibers were found to be more than twice as large as the interior crystallites.

INTRODUCTION

Reusable surface insulation (RSI) is a prime candidate for use as a major portion of the re-entry heat shield on the Space Shuttle orbiter. In this application, it should be

useful for 100 missions in areas where the maximum temperature is expected to reach about 1350⁰ C, for about 20 minutes or less per mission. By rigidizing a very low density felt of ceramic fibers, very lightweight heat shield tiles having low thermal conductivity can be produced. These tiles may be bonded on the primary structure or onto intermediate lightweight support panels. Both mullite (3Al₂O₃-2SiO₂) fibers and silica (SiO₂) fibers are being considered for use in RSI. Silica RSI has a lower thermal conductivity than mullite. However, mullite has a higher use temperature potential and no disruptive phase changes as can occur in silica. Some recently reported properties of mullite tiles are as follows (ref. 1):

Density, kg/m ³	192 to 240
Longitudinal tensile strength, N/m ²	5.9×10 ⁵ to 6.6×10 ⁵
Transverse tensile strength, N/m ²	1.9×10 ⁵ to 2.5×10 ⁵
Tensile strain (to failure), percent	0.17 to 0.23
Thermal expansion per ⁰ C	5.0×10 ⁻⁶
Thermal conductivity (at 1000 ⁰ C and 1.01×10 ⁵ N/m ² pressure), W/(m)(⁰ C)	1.0 to 1.5

Although considerable effort has been directed to the consolidation of mullite fibers into rigidized tiles, little work has been directed toward the characterization of the microstructure of mullite fibers either alone or in the rigidized tiles. It would seem that microstructural features would certainly control the properties of the fibers which in turn should, to some degree, affect the properties of the finished tiles. Thus, it was the purpose of this investigation to examine methods which could more fully reveal the microstructure of mullite fibers. The methods found effective during this study will be used in a subsequent investigation relating microstructural features to mechanical behavior. The ultimate goal is to define what directions to take in improving the mechanical behavior and thermal stability of mullite fibers.

The approach taken in this phase of the effort was to examine a number of mullite-composition fibers and their precursor solution in the as-prepared condition and after subjecting them to a range of thermal exposures, primarily near the maximum end of their useful temperature range. The idea was to ascertain how well various transmission electron microscopy (TEM) techniques could identify microstructural features associated with compositional differences, variations in heat treatments, and differences in material preparation. The experimental techniques used for this purpose included TEM examinations of microtomed sections of mounted fibers and of replicas of polished, chemically etched, and cathodically etched fibers. In addition to the electron microscopy effort, X-ray diffraction analyses were used to identify crystalline phases and to determine crystallite size.

MATERIALS

The materials studied in this investigation are listed in table I(a). Both the spun fibers and monofilaments were supplied by the manufacturer producing the mullite fibers which are being used in the preparation of RSI. The handmade fibers and the cast solution were prepared at Lewis Research Center from the manufacturer's precursor solution.

Description

Of the three spun fibers, the standard fiber is presently being used for making tiles of mullite RSI. According to the phase diagram of the Al_2O_3 - SiO_2 system, figure 1 (ref. 2), the composition of the standard spun fiber should be in the two-phase region of corundum plus mullite at equilibrium. The advantage of being on the Al_2O_3 -rich side of the mullite phase is to ensure a high melting point product. The eutectic temperature here is 1840°C compared to 1595°C on the SiO_2 -rich side. Small amounts of B_2O_3 and P_2O_5 were added during fiber formation to all the materials listed in table I(a) to serve as grain growth inhibitors (refs. 3 and 4) and also to serve as mineralizers (refs. 3 and 4), that is, to promote the formation of mullite. The spun fibers listed as Al_2O_3 -rich and as SiO_2 -rich were included in this study in an attempt to distinguish microstructural features due to chemistry differences. The monofilaments, the handmade fibers, and the cast-precursor solution were included in order to distinguish any possible microstructural effects resulting from preparation differences.

Preparation

The materials listed in table I(a) were all prepared from precursor solutions supplied by the fiber manufacturer. These were made by adding aluminum metal, colloidal silica, boric acid, and phosphoric acid in the proper amounts to either concentrated inorganic acids or inorganic acid salts or both (ref. 5). The concentrated aqueous solution was evaporated to a suitable viscosity for making fibers. Spinning the viscous solution through small orifices by centrifugal force, yielded highly tangled and curly fibers. The monofilaments were produced by pressure extrusion of the precursor solution through a single orifice and by collecting the green fiber on a rotating drum. This process yielded long, straight fibers of uniform diameter. Both the spun and monofilament green fibers were rapidly fired in a tunnel kiln at 1065°C to remove volatiles and to convert the hydrous fibers to the oxides. More details of the fiber manufacturing technique are given in reference 6.

The handmade fibers were produced at NASA Lewis Research Center using the precursor solution of standard composition. A small amount of solution was transferred to a beaker and placed into an ultrasonic bath to ensure uniform mixing. A few drops were then placed on a glass slide and evenly distributed by lightly pressing with a cover slide. The two slides were then pulled apart in rapid motions in front of an electric fan. This process yielded curly but untangled fibers that were instantly dried by the fan. The handmade fibers were not fired as part of their preparation.

The cast material was also prepared at Lewis using the standard composition precursor solution. After ultrasonic mixing, a few drops of the solution were placed on a platinum sheet and evenly distributed to a thin film by lightly pressing with a glass slide. The film was then placed in a platinum crucible and heated to 177°C . This drying treatment was followed by a 10-minute heat at 1065°C in order to convert the hydrous ingredients to the oxide.

Properties

Table I(a) also lists the crystalline phases of the as-prepared materials and the mean fiber diameter of the three spun fibers based on a log normal distribution. The mean diameter values were determined from measurements on 100 fibers from each of the three compositions using a split-image eyepiece mounted on a light microscope. The data were fitted on probability paper and the log normal distribution was found to give the best fit.

EXPERIMENTAL PROCEDURES

Thermal Exposures

The samples studied in this investigation were subjected to various isothermal exposures at 1205°C and at 1426°C . The specimens were heated on platinum foil in a platinum wound furnace and cooled in air. Table I(b) lists the times at temperature for the various materials. The 116-hour exposure of the standard spun fibers consisted of two separate firings, the first lasted 16 hours and the second was for 100 hours.

Specimen Preparation for Transmission Electron Microscope Examination

Thinning procedures. - An ultramicrotome instrument was used to section the fibers for transmission electron microscopy. The fibers were vacuum encapsulated in epoxy

resin. After curing, the specimen block was tapered to the shape of a truncated pyramid 0.1 square millimeter at the tip. The embedded fibers were sectioned with a diamond knife at a cutting angle of 50° . The cut sections (0.3 to 1.5 μm thick) were dropped into water, collected on a carbon covered microscope grid and then were examined.

Mounting, polishing, and chemical etching procedures. - A bundle of fiber (spun or monofilament) was lined up in more or less one direction and placed on a flat metallic surface. A mixture of epoxy resin and a small amount of red dye was poured over the fibers. The dye was used to facilitate detection of the colorless fibers. The resin cured into a flat button shape which was then cut in half, perpendicular to the fibers' axes. The imbedded fibers were again mounted such that the cross section of the fibers were exposed for polishing and etching. The mounted fibers were ground and polished by using wet abrasive papers and 3- and 1/2-micrometer diamond polishing compounds. The fibers were examined as-polished and after chemically etching. The etchant consisted of 90 parts lactic acid, 10 parts nitric acid, and 5 parts of hydrofluoric acid.

Two-step carbon replication. - The mounted and polished samples were replicated in a conventional two-step process with 0.25 percent Mowital in chloroform backed with 2 percent Parlodin in amyl acetate. The replica was shadowed at an angle of 30° with platinum and reinforced with a layer of carbon 100×10^{-10} meter (100 Å) thick. The Mowital and Parlodin layers were dissolved away leaving a negative replica of the fibers.

One-step carbon replication. - Unmounted fibers, either unetched or cathodically etched (see next section), were shadowed with platinum-carbon at an angle of 23° and reinforced with a carbon layer of about 200×10^{-10} meter (200 Å) thick. The coated sample was covered with a thin layer of paraffin to protect the brittle carbon film during the chemical dissolution of the fibers in 30 percent hydrofluoric acid. The paraffin was then removed by heating in distilled water at about 60°C . The last traces of the paraffin were removed by a toluene wash.

Cathodic etching. - The fibers were individually separated and placed on aluminum foil which covered an aluminum block in a cathodic etching apparatus. The aluminum block (and the foil) served as the cathode and the walls of the cathodic etcher served as the anode. The chamber was evacuated to less than 0.66 N/m^2 (5×10^{-3} torr) and flushed twice with argon. Then the argon flow and pumping speed were regulated until a steady pressure of 19.95 N/m^2 (0.15 torr) was obtained. A potential of 2000 volts (5 mA) was applied and held for 5 minutes. The sample was then allowed to cool for 5 minutes after which the potential was reapplied. This cycle was repeated six times for a total etching time of 30 minutes. This sequence achieved the required sample etch without excessive heating of the fibers or of the aluminum backing.

X-Ray Diffraction Procedures

Crystallite size determination. - Crystallite size was determined from diffraction broadening using a diffractometer with a laterally viewed focal spot, Soller slits, and CuK_α radiation. Profiles of specific reflections were made at a scanning speed of $1/4^\circ$ per minute and their breadths were measured at half-maximum peak height. A quartz sample was used as a standard to correct for instrumental broadening. The diffraction profiles measured were the (400) reflection of $\gamma\text{-Al}_2\text{O}_3$ along with the (201) quartz reflection and the (110) reflection of mullite with the (100) quartz reflection. The average crystallite size was calculated from the formula (ref. 7):

$$D_{hkl} = \frac{0.9 \lambda}{\beta_{1/2} \cos \theta}$$

where

D_{hkl} effective thickness of crystallite in direction perpendicular to reflecting planes (hkl)

0.9 constant related to way in which β and D are defined

λ X-ray wave length

$\beta_{1/2}$ pure X-ray diffraction broadening at half-maximum peak height

θ Bragg angle

The pure X-ray diffraction broadening β was calculated from the ratio of the measured breadths of the standard to the sample and the "low angle reflections" correction curve of Klug and Alexander (their fig. 9-8 on p. 509, ref. 7).

Phase identification. - An X-ray diffractometer with CuK_α radiation was used to identify the crystalline phases of ground specimens of the as-prepared and heat treated materials.

RESULTS AND DISCUSSION

The combination of TEM techniques revealed significant facts about the microstructure of the mullite materials tested. These results are discussed hereinafter in terms of each of the experimental techniques used.

Microtome Sections of Mounted Fibers

Microtomed sections were prepared of the three spun fibers only. The fibers were examined in the as-received condition and after two thermal exposures of 1 and 16 hours at 1426°C . All three of the as-received fibers were found to consist of extremely small crystallites (about 100×10^{-10} to 200×10^{-10} m or 100 to 200 Å) dispersed in a large amount of an amorphous phase. The structure shown in figure 2 is representative of the fiber sections from all three compositions. Because of the brittle nature of the fibers, the sectioning process resulted in nonuniformly thick sections with some parts too thick for electron transmission. The crystallites in the thinner parts can be seen as small dark shapes with sharp edges dispersed in a formless gray area which is the amorphous phase. The only crystalline phase detected by X-ray diffraction (table I) in the as-received standard fibers and in the Al_2O_3 -rich fibers was $\gamma\text{-Al}_2\text{O}_3$. And mullite was the only crystalline phase detected in the as-received SiO_2 -rich fibers. Because the crystallites were so small the two crystalline types could not be distinguished by viewing the photomicrographs.

After heating the fibers at 1426°C for 1 and 16 hours the crystallites increased in size and the amount of amorphous phase decreased. Figures 3 and 4 are representative photomicrographs of the thermally exposed spun fibers. The gray areas between the crystallites is the amorphous phase. After the 1426°C treatments, mullite was the only phase detected by X-ray diffraction (table I) in all three of the spun fibers. Thus all the crystallites in figures 3 and 4 are assumed to be mullite. These crystals are elongated polyhedra, some of which are oriented such that their short axes are in the plane of the photo giving them a square appearance. A prismatic crystalline habit is expected here since this mullite was produced essentially from heating the component oxides together (ref. 8). The more common acicular morphology is present only when the mullite is formed in the presence of a liquid phase, such as in solidification from the melt (ref. 8).

Table II lists the crystallite size determined by measuring the widths of the crystallites appearing in the transmission photos and compares these values to those determined by X-ray diffraction. For each electron microscope value given in table II about 100 measurements were taken. A comparison of the two sets of values shows good agreement. Both sets of values show that, with the standard spun fibers and the Al_2O_3 -rich spun fibers, the average size increased until the 16-hour, 1426°C exposure where the average size decreased. For the SiO_2 -rich spun fibers the size at first increased and then remained more or less constant between the 1-hour, 1205°C and the 1-hour, 1426°C exposures and then it increased again. The observed discontinuity in growth can be explained by assuming that during the series of thermal exposures new crystallites are being nucleated from the amorphous phase while those already present continue to grow. The smaller, more recently nucleated crystallites eventually become sufficient

in number so as to bias the average to a lower value despite the increase in size of the original crystallites. The temperature at which this concurrent nucleation and growth process causes a discontinuity in the average growth rate was found to be higher for the standard and the Al_2O_3 -rich fibers than for the SiO_2 -rich fibers. This temperature relation is probably due to the fact that the homologous temperature of the standard and the Al_2O_3 -rich fibers is higher than that of the SiO_2 -rich fibers.

The concurrent nucleation and growth process should result in a rather large range of crystallite sizes in the thermal exposed specimens. Indeed such a large size range was evident in measurements from TEM photos. For example after 1 hour at 1426°C the SiO_2 -rich fibers with an average size of 350×10^{-10} meter (350 \AA) had a size range from about 200×10^{-10} to 800×10^{-10} meter (200 to 800 \AA).

Experimental proof of the concurrent nucleation and growth phenomenon was sought. Standard spun fibers were heated to 1426°C for 1 hour, then leached in hydrofluoric acid for 10 minutes. The purpose of the acid treatment was to preferentially dissolve the amorphous phase and thereby decrease substantially the amount of nucleation possible thereafter. The fibers were then reheated at 1426°C for an additional 15 hours and then subjected to X-ray diffraction analysis. Again mullite was the only phase detected in this specimen and the average crystallite size was beyond the limits of detection by the X-ray line broadening technique, that is, $>2000 \text{ \AA}$.

Finally a standard fiber specimen which was previously heated at 1426°C for 16 hours was fired an additional 100 hours at this temperature. The purpose was to allow time for the completion of the nucleation process and to allow large crystals to grow. Table II lists the size data on this specimen as 1350 \AA as determined from X-ray and as 1022 \AA as measured from many photomicrographs. Figure 5 is representative of those photos. It is interesting to note that, even after such a relatively long exposure, the average crystallite size is still less than that of the acid leached specimen. This observation suggests that, even after long times at temperature, the nucleation of new crystallites from the remaining amorphous phase is still significant. Also important is the fact that the standard fiber after 116 hours at 1426°C has an average crystallite size much less than the mean fiber diameter of 6.8 micrometers. Thus, the degradation of mechanical properties observed in these fibers after being exposed to temperatures of 1325°C and higher (ref. 4) is not the result of the crystallites growing to the dimension of the fiber's diameter as has been proposed in the case of Y_2O_3 -stabilized ZrO_2 fibers (ref. 9).

Replicas of Unetched Fibers

A limited number of surface replicas of unetched fibers were examined. One of the specimens so examined was the standard spun fiber which was exposed for 16 hours at

1426° C and then heated an additional 100 hours at the same temperature. Its surface microstructure as seen in figure 6 shows large crystallites with facets clearly resolved. The crystallites are essentially contiguous with no apparent amorphous phase. The crystallites are sufficiently large to be seen in the scanning electron microscope, although the facets are not resolved as shown in figure 7. The mullite fiber X-ray diffraction pattern contains mullite lines as expected and a few unidentified lines. The average surface grain width as measured from the electron photomicrographs is 2300×10^{-10} meter (2300 Å) compared to an X-ray value of 1350×10^{-10} meter (1350 Å) and to 1022×10^{-10} meter (1022 Å) from measurements from the transmission photos (table II). The replica shows essentially the surface structure while the electron transmission is more representative of the internal structure. Thus, after an exposure of at least 116 hours at 1426° C, the outer crystallites are larger than the internal crystallites.

Replicas of Polished and Chemically Etched Fibers

The amount of internal porosity is an important factor in the fiber strength. For this reason it was important to see if the amount of internal porosity could be observed in these small diameter fibers. For this purpose the standard spun fibers, the as-received monofilaments, and the monofilaments after exposure to 1205° C for 1/2 hour were mounted and polished as described earlier. The cross sections of these fibers are shown in figures 8, 9, and 10. Figure 8 shows the as-received standard spun fiber. No indication of porosity is seen here although there is a faint indication of some structure. Figure 9 shows the as-received monofilament. Very little internal porosity can be observed. Figure 10 shows the monofilament after a moderate thermal exposure and again very little internal porosity can be seen. These observations are in direct contrast to those in reference 3 where 10 to 20 volume percent porosity was reported. The technique used in reference 3 was the replication of fractured fiber surfaces. Beyond showing features related to fracture such replicas are difficult to interpret. It would appear that the examination of a replica of a polished surface is more informative for porosity determinations.

An important observation here is that it was possible to obtain polished surfaces of good quality even though the size of the abrasive used ($1/2$ - μ m diamond) was relatively large compared to the diameter of the fiber (6.8 μ m).

Chemical etching of the cross section of the polished as-received fibers revealed no useful metallographic information. Figure 11 is a typical example. The only features seen are the many small areas that have been preferentially attacked by the etchant. (In negative replicas the depressions appear as mounds when viewed from the direction of the shadowing.) These etched out areas roughly range in size from 400×10^{-10} to 2000×10^{-10} meter (400 to 2000 Å). Although their appearance is similar to etch pits,

they are not believed to be etch pits since they are much larger than the crystallites (100×10^{-10} to 200×10^{-10} m or 100 to 200 Å). The interpretation of these features is not fully understood at this time. However, they may be related to features revealed by cathodic etching (discussed hereinafter). No attempt was made to chemically etch thermally exposed fibers since the feasibility of obtaining information by chemically etching mullite fibers when containing large crystallites (about 1000×10^{-3} m or 1000 Å or larger) has already been demonstrated (ref. 3). However, a study to optimize etchant composition or etching technique would be worth further consideration in order to be able to distinguish different phases and to reveal more clearly crystallites of sizes below 1000×10^{-3} m (1000 Å).

Replicas of Cathodically Etched Materials

Samples from all the materials studied during this investigation (as-prepared and thermally exposed) were cathodically surface etched and replicated. The major findings from the examination of surface replicas of the spun fibers are as follows: The standard composition fibers and the Al_2O_3 -rich fibers displayed similar features which consisted of cellular surface structures (fig. 12) and striations (fig. 13). Over the surface of any fiber the structure is inhomogeneous with cells and striations sometimes appearing together and with cell size varying along the fiber. Curiously, the features revealed by cathodic etching seem unaffected by thermal exposure or phases present (crystalline to noncrystalline). Thus the as-received fiber shown in figure 12 cannot be readily distinguished from the heat treated fiber in figure 14. Further the dimensions of the structural features of the cathodically etched fibers cannot be correlated with the crystal size calculated from X-ray diffraction or measured from electron microscope photos.

In figures 12, 13, and 14 there is a small amount of intercellular surface area which differs in appearance from the rest of the structure. Its appearance might suggest a separate phase. But X-ray results do not confirm this interpretation. Another possibility is that these features are the result of shadowing differences caused by the varying depths of the indentations in the replica.

The SiO_2 -rich fibers also contained the cellular structure but striations were never observed. The SiO_2 -rich fibers differed from the standard and the Al_2O_3 -rich fibers in two other respects. One is the frequent appearance of a tiered structure as seen in figure 15. The other is the occasional appearance of a structure in the thermally exposed fibers that looks as if it had been molten at temperature (fig. 16).

The distinctive features revealed by surface cathodic etching appear real but they cannot be related for the most part to composition or exposure. It is possible then that this technique is not revealing structure on the scale of the crystallite size but it may be revealing features of a larger size. These larger features may be caused by fiber

processing and thus reflect processing history. For example, the striations in figure 13 may be related to the shearing that must be present when the precursor solution is forced through the spinnerette orifice and rapidly dried. Such striations were also observed in monofilaments and the handmade fibers, again suggesting the action of shearing forces during processing. On the basis of this rationale an effort was made to see if the microstructural features resulting from cathodic etching could be related to processing differences. For this purpose the three spun fibers, the monofilament, the handmade fibers, and the cast-precursor solution were tested. The preparation of these materials differed with respect to many of the important processing parameters such as the basic forming mode (drawn, spun, or cast), humidity, drying method, collection mode and firing schedule, and so forth.

The as-prepared cast precursor solution (fired during preparation for 10 min at 1065°C) did indeed have a unique structure as seen in figure 17. However, after a thermal exposure at 1426°C the cast material developed cellular structures similar to those of the spun fibers (see fig. 18). The cathodically etched monofilament and the handmade fibers could not be distinguished from the spun fibers either in the as-prepared condition or after thermal exposure.

Thus, this cursory examination did not demonstrate the ability of cathodic etching to differentiate processing parameter differences among the fibers. Nevertheless, the very distinctive features revealed by this etching method must be associated with some aspect of the microstructure of these fibers. Perhaps a more systematic study with well-controlled processing parameters may reveal a relation between the features exposed by cathodic etching and the processing parameters. If indeed it does, then cathodic etching would prove to be a useful tool for studying the effects of processing variables upon fiber properties.

That the microstructure is sensitive to processing parameters can be demonstrated by the X-ray results in table II. In the extreme case of the cast-precursor solution and the standard spun fiber, as an example, the crystalline phase in the as-prepared cast solution is mullite with an average size of 440×10^{-3} meter (440 \AA) compared to $\gamma\text{-Al}_2\text{O}_3$ in the fiber with an average size of 61×10^{-10} meter (61 \AA). After an exposure of 16 hours at 1426°C the crystalline phase is mullite in both materials but the average crystallite size is (1380 \AA) for the cast solution (about a threefold increase) and 378×10^{-10} meter (378 \AA) for the fiber (about a sixfold increase). Similar comparisons are possible among the fibers. Thus such features as crystalline phase and crystallite size are sensitive to processing differences and these differences affect the growth process of the crystallites during thermal exposure.

SUMMARY OF RESULTS

In this investigation the microstructures of mullite-composition fibers were examined by a number of transmission electron microscopy techniques and by X-ray diffraction. Three compositions were evaluated; the standard composition was slightly Al_2O_3 -rich, while the other compositions were highly Al_2O_5 -rich and SiO_2 -rich. The major findings are as follows:

The as-received fibers of standard composition, both the spun and the monofilament contained little if any internal porosity. Nor did the degree of porosity change after heating the monofilament for 1/2 hour at 1205°C . Prior to the thermal exposures, the crystallites in all three of the spun fibers were very small (about 100 to 200 Å) and were dispersed in a large amount of an amorphous phase. When thermally exposed, these crystallites grew and simultaneously new crystallites were nucleated from the amorphous phase. After sufficient time at temperature (e. g., 116 hr at 1426°C), the crystallites of the standard spun fibers became contiguous. At this juncture the average crystallite size was less than 0.2 micrometer, relatively small compared to the mean fiber diameter of 6.8 micrometers. In addition, the surface crystallites of these fibers were found to be more than twice as large as the interior crystallites.

CONCLUDING REMARKS

The primary objective of this study was to find transmission electron microscopic methods which could more fully reveal the microstructure of mullite fibers of the type used in the preparation of reusable surface insulation (RSI). A combination of techniques was found to yield most of the desired information. Thus electron transmission microscopy of microtomed sections proves useful in showing individual crystalline material. Replicas of polished and unetched cross sections readily revealed the extent of porosity, and replicas of thermally exposed fibers were useful for observing the surface crystallites. Replicas of cathodically etched fibers were interesting in that they showed very distinct features that appeared to be real. Such features, however, could not be related, for the most part, to fiber composition or thermal exposure. There is some indication that the observed features are related to the processing history of the fibers. Therefore, a systematic study relating structural features revealed by cathodic etching to well-controlled processing parameters could prove worthwhile.

Thus, by the proper combination of a number of transmission electron microscopy techniques a valuable description of the microstructure of mullite fibers can be obtained.

The potential for such a microstructural description is, of course, to ultimately relate fiber microstructure to mechanical behavior and thermal stability.

Lewis Research Center,
National Aeronautics and Space Administration,
Cleveland, Ohio, December 1, 1972,
502-31.

REFERENCES

1. Goldstein, Howard E.; Buckley, John D.; King, Harry M.; Probst, Hubert B.; and Spiker, Ivan K.: Reusable Surface Insulation Materials Research and Development. NASA Space Shuttle Technology Conference - Dynamics and Aeroelasticity; Structures and Materials. NASA TM X-2570, 1972, pp. 373-433.
2. Aramaki, Shigeo; and Roy, Rustrum: Revised Phase Diagram for the System Al_2O_3 - SiO_2 . J. Am. Ceram. Soc., vol. 45, no. 5, May 1962, pp. 229-242.
3. Fetterolf, Robert N.: Development of High Strength, High Modulus Fibers. Rep. B/W-7953, Babcock and Wilcox Co. (AFML-TR-70-197, AD-875583L), Aug. 1970.
4. Fetterolf, R. N.: Development Studies on Mullite Fiber. Rep. 5159, Babcock and Wilcox Co. (NASA CR-120929), 1971.
5. Fetterolf, R. N.: Development of a High Strength, High Modulus Ceramic Fiber. Rep. 5144, Babcock and Wilcox Co. (NASA CR-98156), Sept. 29, 1968.
6. Blaze, Joseph E., Jr.: High Temperature Al_2O_3 - SiO_2 Fibers and Methods of Manufacture. Patent No. 3,503,765, United States, Mar. 1970.
7. Klug, Harold P.; and Alexander, Leroy E.: X-ray Diffraction Procedures for Polycrystalline and Amorphous Materials. John Wiley & Sons, Inc., 1954.
8. Davis, Robert F.; and Pask, Joseph A.: Mullite. High Temperature Oxides. Part 4 - Refractory Glasses, Glass-Ceramics, and Ceramics. Allen M. Alper, ed., Academic Press, 1971, pp. 37-76.
9. Tanzilli, Richard A., ed.: Development of an External Ceramic Insulation for the Space Shuttle Orbiter. General Electric Co. (NASA CR-112038), Apr. 1972.

TABLE I. - MATERIALS STUDIED

(a) As-prepared

Materials	Composition, molecular percent (wt. %)				Crystalline phases	Mean fiber diameter (log-normal distribution), μm
	Al_2O_3	SiO_2	B_2O_3	P_2O_5		
Standard spun fiber	67.7 (77.0)	25.5 (17.0)	5.8 (4.5)	1.0 (1.6)	$\gamma\text{-Al}_2\text{O}_3$	6.8 ± 4.0
Al_2O_3 -rich spun fiber	77.4 (84.0)	15.8 (10.1)	5.8 (4.3)	1.0 (1.5)	$\gamma\text{-Al}_2\text{O}_3$	9.5 ± 2.1
SiO_2 -rich spun fiber	53.2 (64.8)	40.0 (28.7)	5.8 (4.9)	1.0 (1.7)	Mullite	8.0 ± 2.5
Monofilament	67.7 (77.0)	25.5 (17.0)	5.8 (4.5)	1.0 (1.6)	Mullite	^a 6.8
Handmade fiber	67.7 (77.0)	25.5 (17.0)	5.8 (4.5)	1.0 (1.6)	Mullite	-----
Cast solution	67.7 (77.0)	25.5 (17.0)	5.8 (4.5)	1.0 (1.6)	Mullite	-----

(b) Thermal exposures

Materials	Time, hr	Temperature, $^{\circ}\text{C}$	Crystalline phases
Standard spun fiber	1	1205	Mullite
Al_2O_3 -rich spun fiber	1	1426	Mullite
SiO_2 -rich spun fiber	16	1426	Mullite
Standard spun fiber	^b 116	1426	Mullite
Monofilament	1/2	1205	Mullite
	1	1205	Mullite
	1	1426	Mullite
Cast solution	1	1426	Mullite plus few unidentified lines
	16	1426	Mullite plus few unidentified lines

^aManufacturer's data - normal average of 10 measurements.

^bHeated for 16 hr at 1425°C , cooled to room temperature, and reheated additional 100 hr at 1426°C .

TABLE II. - CRYSTALLITE SIZE

Materials	Treatment	Type of photo-graph	Electron microscope size (width)		X-ray diffraction		
			m	Å	Size		Phases
					m	Å	
Standard spun fiber	As-received	Transmission	100×10^{-10} to 200×10^{-10}	~100 to 200	61×10^{-10}	61	γ - Al_2O_3
	1 hr at 1205°C	-----	-----	-----	423×10^{-10}	423	Mullite
	1 hr at 1426°C	Transmission	663×10^{-10}	663	765×10^{-10}	765	Mullite
	16 hr at 1426°C	Transmission	480×10^{-10}	480	378×10^{-10}	378	Mullite
	16 hr at 1426°C + cooled to room temperature + 100 hr at 1426°C	Transmission	1022×10^{-10}	1022	1350×10^{-10}	1350	Mullite + ?
Al_2O_3 -rich spun fiber	16 hr at 1426°C + cooled to room temperature + 100 hr at 1426°C	Replica	2300×10^{-10}	2300	1350×10^{-10}	1350	Mullite + ?
	1 hr at 1426°C + leach in hydrofluoric acid at room temperature + 15 hr at 1426°C	-----	-----	-----	$>2000 \times 10^{-10}$	>2000	Mullite
	1 hr at 1205°C + leach in hydrofluoric acid at room temperature + 16 hr at 1426°C	Replica	1300×10^{-10}	1300	1370×10^{-10}	1370	Mullite + few α - Al_2O_3 lines
	As-received	Transmission	$\sim 100 \times 10^{-10}$ to 200×10^{-10}	~100 to 200	73×10^{-10}	73	γ - Al_2O_3
	1 hr at 1205°C	-----	-----	-----	345×10^{-10}	345	Mullite
SiO_2 -rich spun fiber	1 hr at 1426°C	Transmission	950×10^{-10}	950	1000×10^{-10}	1000	Mullite
	16 hr at 1426°C	Transmission	520×10^{-10}	520	838×10^{-10}	838	Mullite
	As-received	Transmission	-----	~100 to 200	213×10^{-10}	213	Mullite
	1 hr at 1205°C	-----	-----	-----	408×10^{-10}	408	Mullite
	1 hr at 1426°C	Transmission	350×10^{-10}	350	325×10^{-10}	325	Mullite
Cast solution	16 hr at 1426°C	Transmission	519×10^{-10}	519	623×10^{-10}	623	Mullite
	As-prepared	-----	-----	-----	440×10^{-10}	440	Mullite
	16 hr at 1426°C	-----	-----	-----	1380×10^{-10}	1380	Mullite + ?

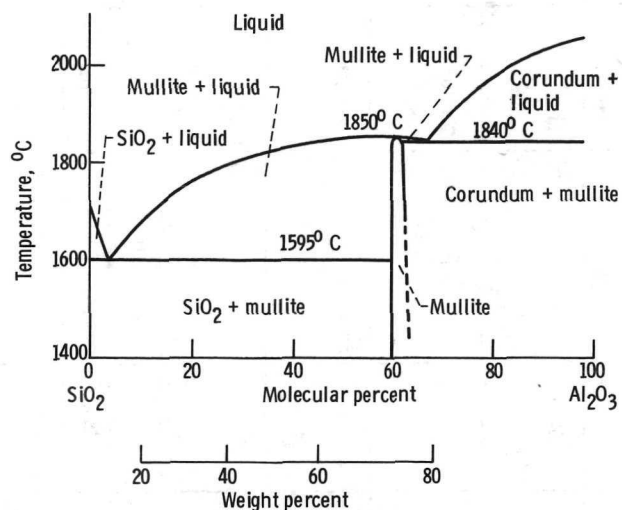


Figure 1. - Al_2O_3 - SiO_2 binary system according to reference 2.



Figure 2. - Microtomed section of as-received standard spun fiber. Crystallites appear as small dark spots dispersed in amorphous phase (gray area).

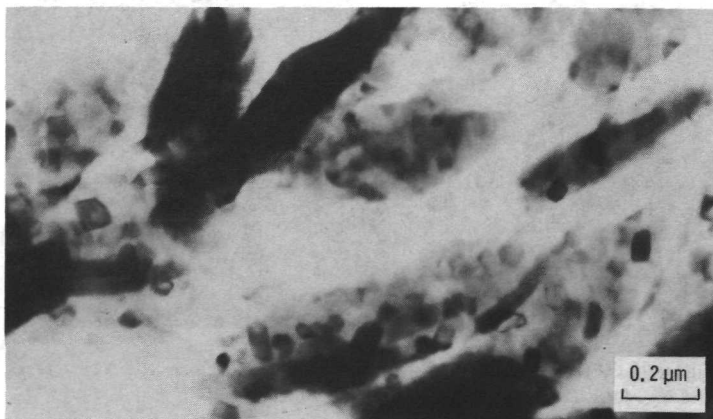


Figure 3. - Microtomed section of SiO₂-rich spun fiber after thermal exposure at 1426° C for 1 hour.



Figure 4. - Microtomed section of SiO₂-rich spun fiber after thermal exposure at 1426° C for 16 hours.



Figure 5. - Microtomed section of standard spun fiber after thermal exposure at 1426° C for total time at temperature of 116 hours.

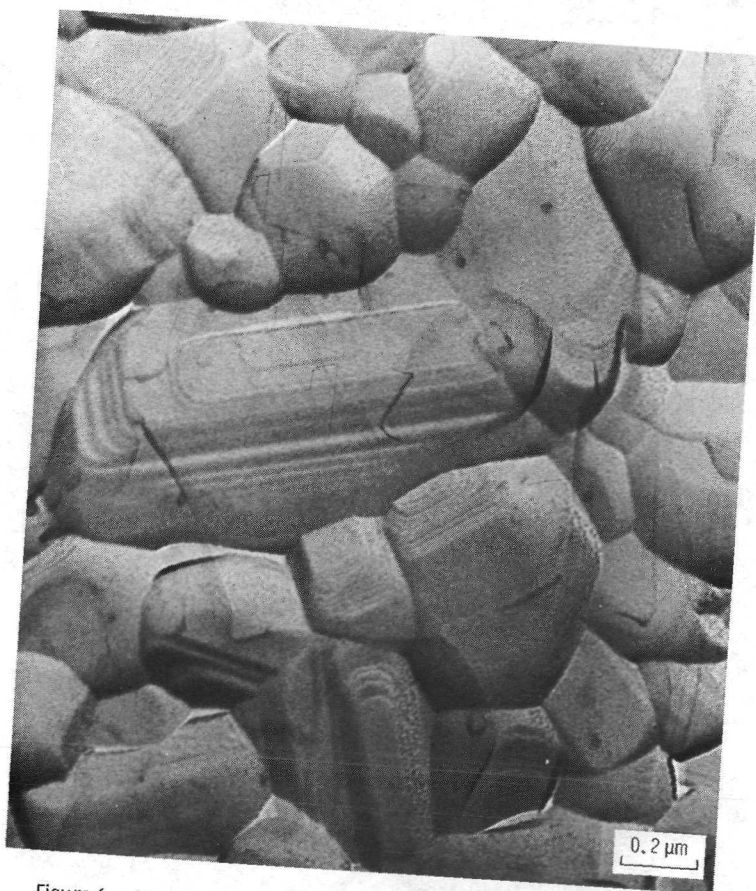


Figure 6. - Unetched replica of standard spun fiber after thermal exposure at 1426° C for total time at temperature of 116 hours.

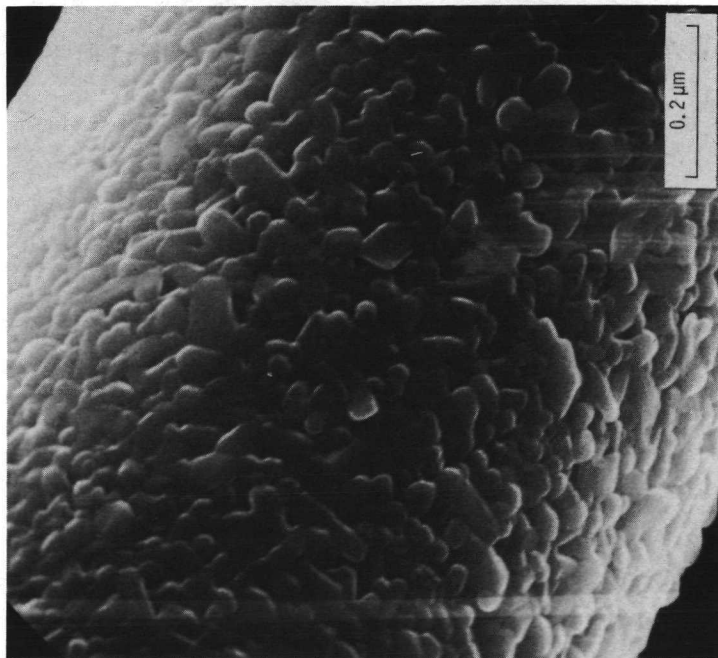


Figure 7. - Scanning electron microscope after thermal exposure at 1426° C for total time at temperature of 116 hours.

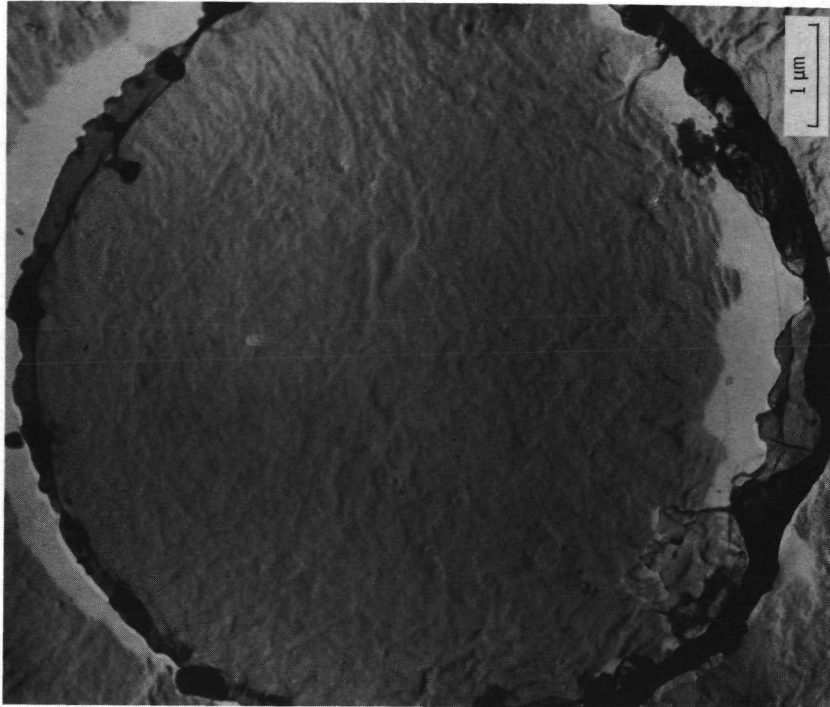


Figure 8. - Polished and unetched cross section of as-received standard spun fiber.

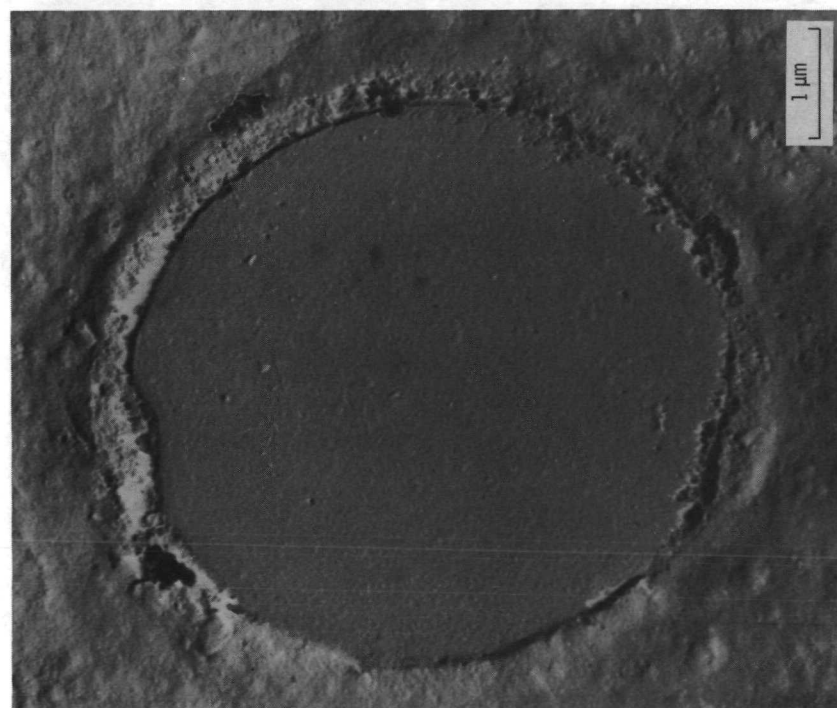


Figure 9. - Polished and unetched cross section of as-received monofilament of standard composition.

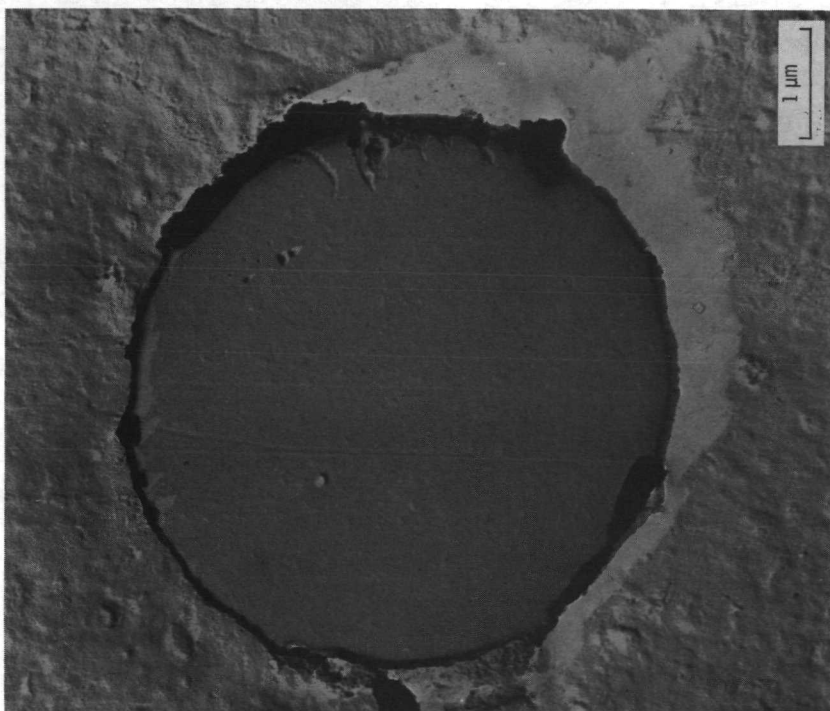


Figure 10. - Polished and unetched cross section of monofilament of standard composition after thermal exposure at 1205° C for 1/2 hour.

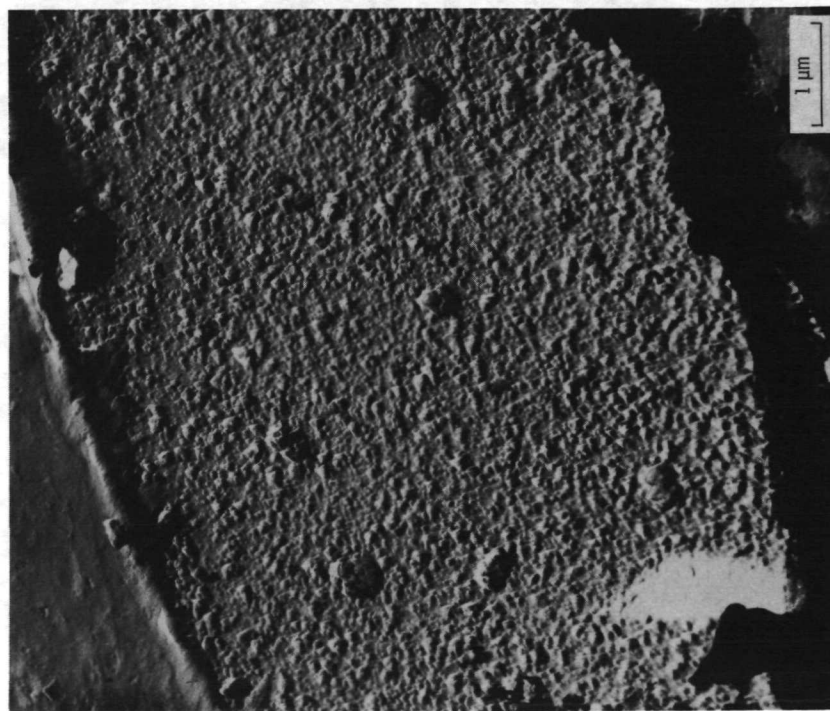


Figure 11. - Chemically etched cross section of as-received standard spun fiber.

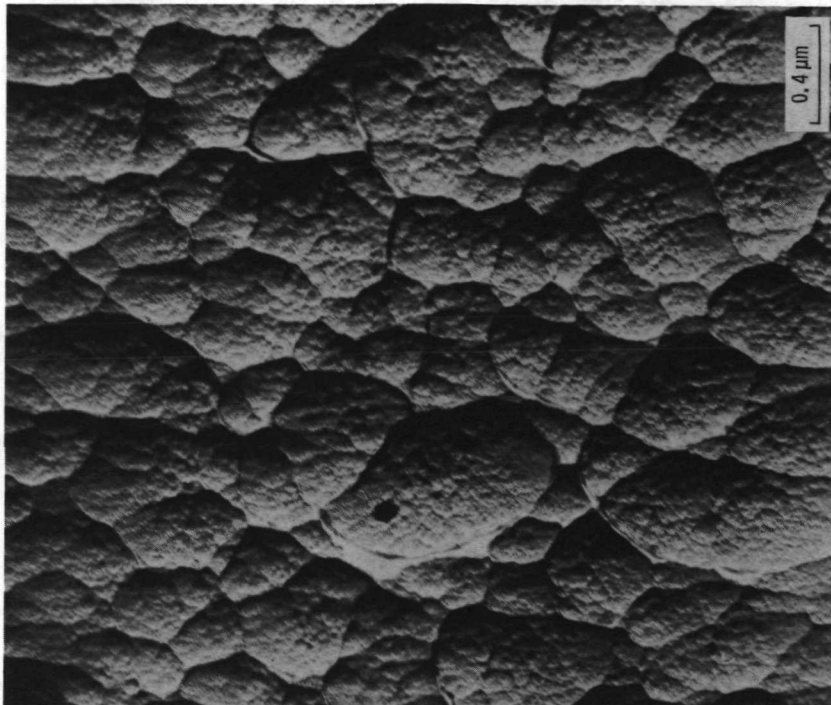


Figure 12. - Cathodically etched surface of as-received standard spun fiber with cellular structure.



Figure 13. - Cathodically etched surface of as-received standard spun fiber with striated structure.

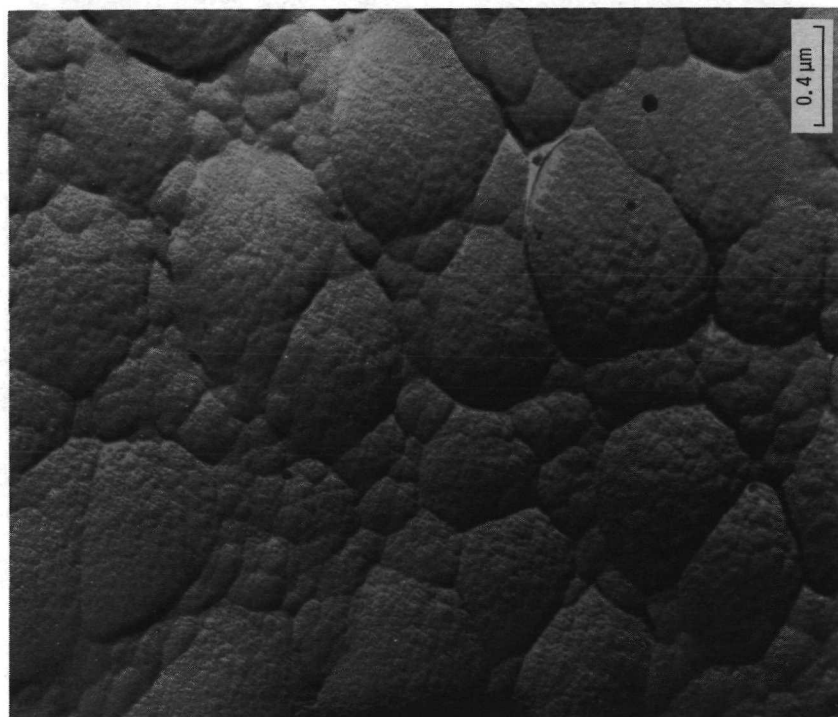


Figure 14. - Cathodically etched surface of standard spun fiber after thermal exposure at 1426°C for 16 hours.

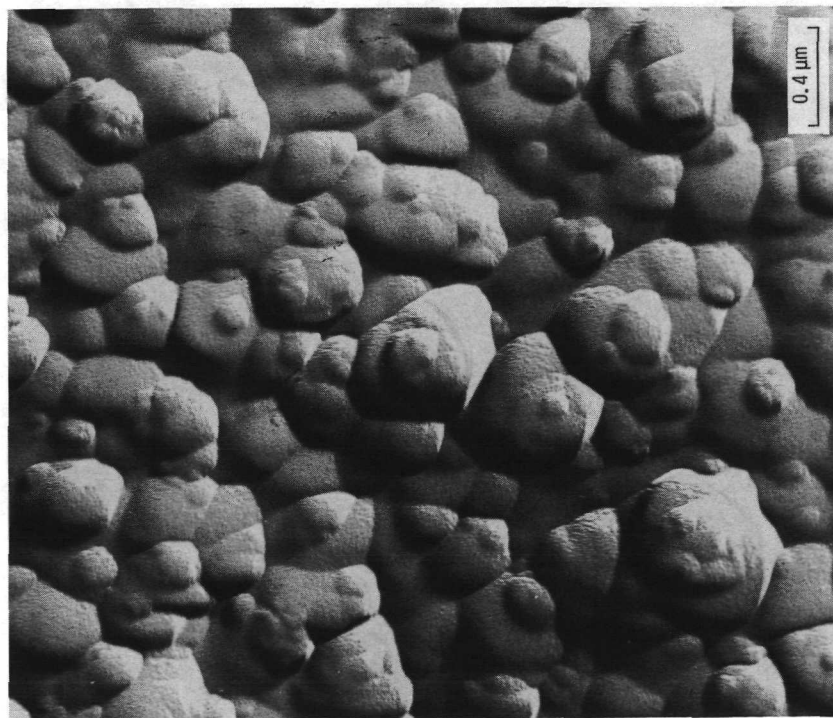


Figure 15. - Cathodically etched surface of as-received SiO_2 -rich spun fiber with tiered structure.

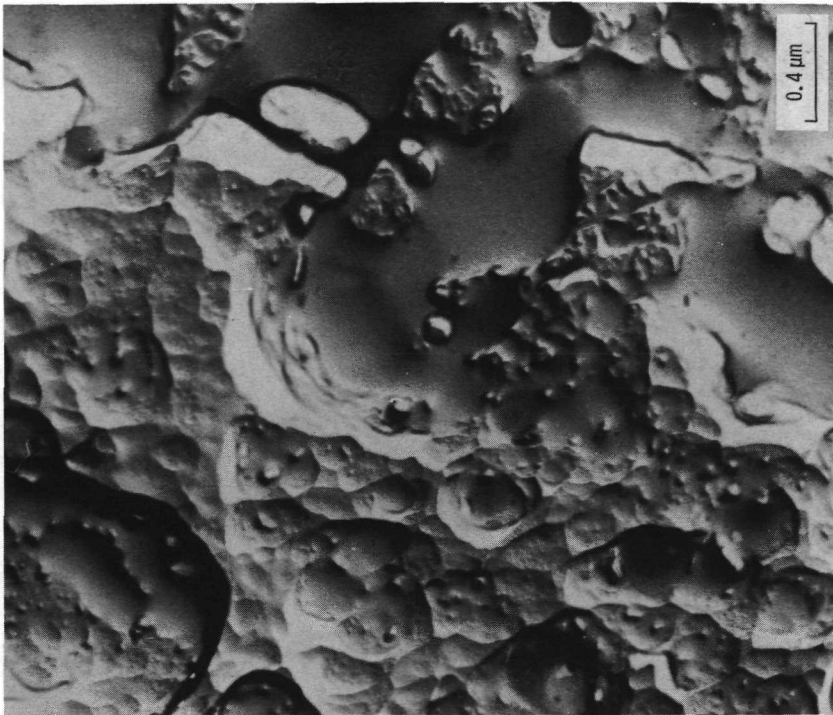


Figure 16. - Cathodically etched surface of SiO_2 -rich spun fiber after thermal exposure at 1426°C for 1 hour.

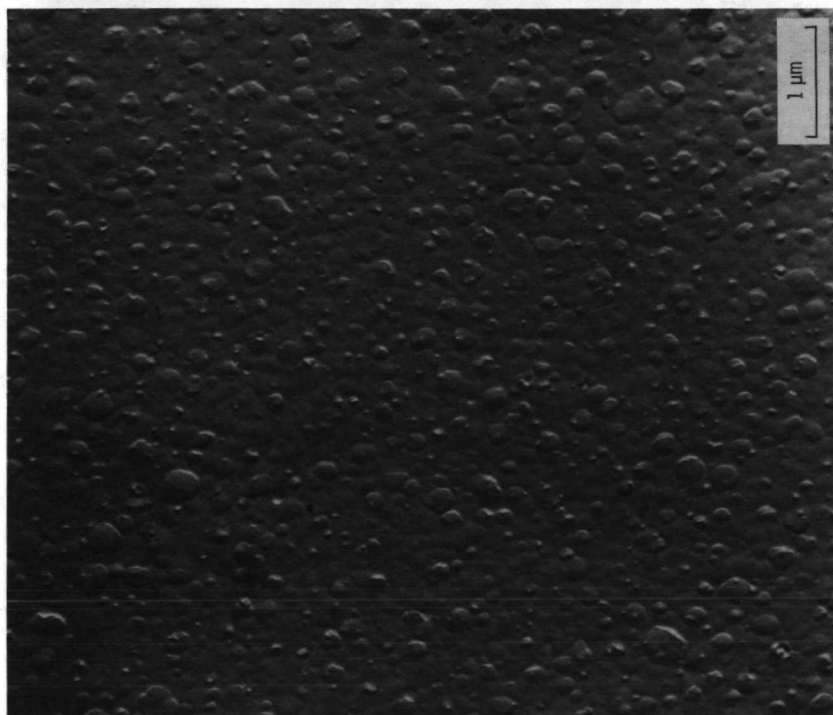


Figure 17. - Cathodically etched surface of as-prepared cast precursor solution of standard composition.

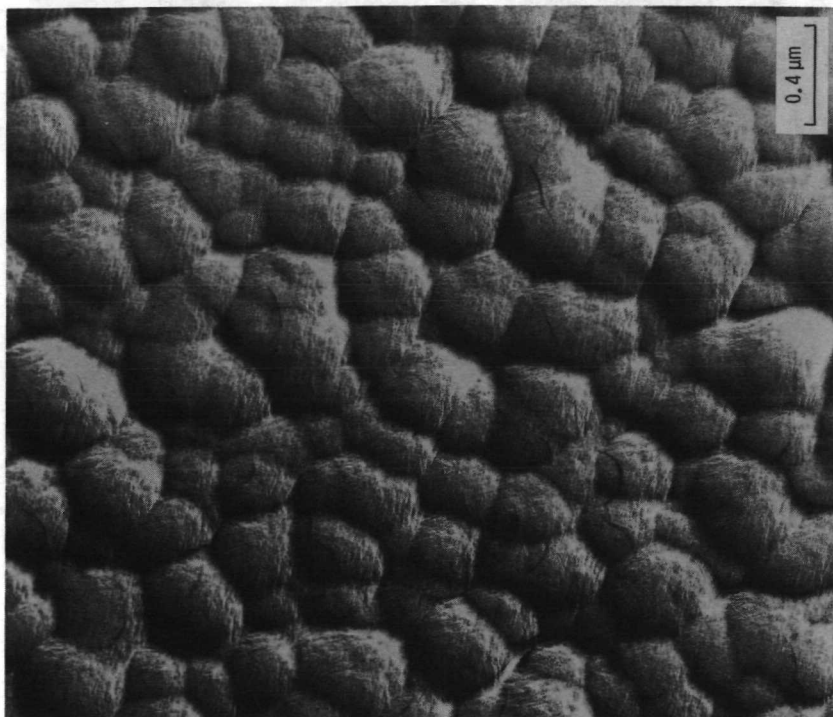


Figure 18. - Cathodically etched surface of cast precursor solution of standard composition after 16 hours at 1426°C.



POSTMASTER: If Undeliverable (Section 158
Postal Manual) Do Not Return

"The aeronautical and space activities of the United States shall be conducted so as to contribute . . . to the expansion of human knowledge of phenomena in the atmosphere and space. The Administration shall provide for the widest practicable and appropriate dissemination of information concerning its activities and the results thereof."

—NATIONAL AERONAUTICS AND SPACE ACT OF 1958

NASA SCIENTIFIC AND TECHNICAL PUBLICATIONS

TECHNICAL REPORTS: Scientific and technical information considered important, complete, and a lasting contribution to existing knowledge.

TECHNICAL NOTES: Information less broad in scope but nevertheless of importance as a contribution to existing knowledge.

TECHNICAL MEMORANDUMS: Information receiving limited distribution because of preliminary data, security classification, or other reasons. Also includes conference proceedings with either limited or unlimited distribution.

CONTRACTOR REPORTS: Scientific and technical information generated under a NASA contract or grant and considered an important contribution to existing knowledge.

TECHNICAL TRANSLATIONS: Information published in a foreign language considered to merit NASA distribution in English.

SPECIAL PUBLICATIONS: Information derived from or of value to NASA activities. Publications include final reports of major projects, monographs, data compilations, handbooks, sourcebooks, and special bibliographies.

TECHNOLOGY UTILIZATION PUBLICATIONS: Information on technology used by NASA that may be of particular interest in commercial and other non-aerospace applications. Publications include Tech Briefs, Technology Utilization Reports and Technology Surveys.

Details on the availability of these publications may be obtained from:

SCIENTIFIC AND TECHNICAL INFORMATION OFFICE

NATIONAL AERONAUTICS AND SPACE ADMINISTRATION

Washington, D.C. 20546